Published for SISSA by Springer

Received: *June 10, 2013*
Revised: *July 31, 2013*
Accepted: *August 14, 2013*
Published: *September 10, 2013*

Constraining Inert Dark Matter by $R_{\gamma\gamma}$ and WMAP data

Maria Krawczyk, Dorota Sokołowska, Paweł Swaczyna and Bogumiła Świeżewska

University of Warsaw, Faculty of Physics,
Hoża 69, 00-681 Warszawa, Poland

E-mail: maria.krawczyk@fuw.edu.pl, dorota.sokolowska@fuw.edu.pl, pawel.swaczyna@student.uw.edu.pl, bogumila.swiezewska@fuw.edu.pl

Abstract: We discuss the constraints on Dark Matter coming from the LHC Higgs data and WMAP relic density measurements for the Inert Doublet Model, which is one of the simplest extensions of the Standard Model providing a Dark Matter candidate. We found that combining the diphoton rate $R_{\gamma\gamma}$ and the $\Omega_{DM}h^2$ data one can set strong limits on the parameter space of the Inert Doublet Model, stronger or comparable to the constraints provided by the XENON100 experiment for low and medium Dark Matter mass.

Keywords: Higgs Physics, Beyond Standard Model

ArXiv ePrint: 1305.6266

doi:10.1007/JHEP09(2013)055

Contents

1 Introduction

Dark Matter (DM) is thought to constitute around 25% of the Universe's mass-energy density, but its precise nature is yet unknown. The DM relic density $\Omega_{DM}h^2$ is well measured by WMAP and Planck experiments and the current value of $\Omega_{DM}h^2$ is [1]:

$$\Omega_{DM}h^2 = 0.1126 \pm 0.0036. \tag{1.1}$$

Various direct and indirect detection experiments have reported signals that can be interpreted as DM particles. Low DM masses $\lesssim 10\,\text{GeV}$ are favoured by DAMA/LIBRA [2], CoGeNT [3, 4] and recently by CDMS-II [5] experiment, while the medium mass region of 25–60 GeV by CRESST-II [6]. All those events lie in the regions excluded by the XENON10 and XENON100 experiments, which set the strongest limits on the DM-nucleon scattering cross-section [7]. There have also been reports of the observation of products of the annihilation of DM particles, including the recent 130 GeV γ-line from the Fermi-LAT experiment [8–10]. However, there is no agreement as to whether one can truly interpret those indirect measurements as a proof of existence of Dark Matter (see e.g. [11, 12] for reviews).

There have been many attempts to explain those contradictory results either by assuming some experimental inaccuracies coming from incorrectly determined physical quantities in astrophysics or nuclear physics, or by interpreting the results in modified astrophysical models of DM (see e.g. [13–17]). However, so far no agreement has been reached, and the situation in direct and indirect detection experiments is not yet clear [12, 16, 18, 19].

In this paper we set constraints on the scalar DM particle from the Inert Doublet Model (IDM), using solely the LHC Higgs data and relic density measurements. The IDM

JHEP09(2013)055

provides an example of a Higgs portal DM. In a vast region of the allowed DM masses, particularly in the range that the LHC can directly test, the main annihilation channel of DM particles and their interaction with nucleons, relevant for direct DM detection, are processed by exchange of the Higgs particle. We found that the $h \to \gamma\gamma$ data for the SM-like Higgs particle with mass $M_h \approx (125 - 126)$ GeV sets strong constraints on the allowed masses and couplings of DM in the IDM. Combining them with the WMAP results excludes a large part of the IDM parameter space, setting limits on DM that are stronger or comparable to those obtained by XENON100.

2 Inert Doublet Model

The Inert Doublet Model is defined as a 2HDM with an exact D (Z_2 type) symmetry: $\phi_S \to \phi_S, \phi_D \to -\phi_D$ [20, 21], i.e. a 2HDM with a D-symmetric potential, vacuum state and Yukawa interaction (Model I). In the IDM only one doublet, ϕ_S, is involved in the Spontaneous Symmetry Breaking, while the D-odd doublet, ϕ_D, is inert, having $\langle \phi_D \rangle = 0$ and no couplings to fermions. The lightest particle coming from this doublet is stable, being a good Dark Matter candidate.

The IDM provides, apart from the DM candidate, also a good framework for studies of the thermal evolution of the Universe [22–25], electroweak symmetry breaking [26], strong electroweak phase transition [27–30] and neutrino masses [31, 32].

The D-symmetric potential of the IDM has the following form:

$$\begin{aligned} V = &-\frac{1}{2}\left[m_{11}^2(\phi_S^\dagger\phi_S) + m_{22}^2(\phi_D^\dagger\phi_D)\right] + \frac{\lambda_1}{2}(\phi_S^\dagger\phi_S)^2 + \frac{\lambda_2}{2}(\phi_D^\dagger\phi_D)^2 \\ &+\lambda_3(\phi_S^\dagger\phi_S)(\phi_D^\dagger\phi_D) + \lambda_4(\phi_S^\dagger\phi_D)(\phi_D^\dagger\phi_S) + \frac{\lambda_5}{2}\left[(\phi_S^\dagger\phi_D)^2 + (\phi_D^\dagger\phi_S)^2\right], \end{aligned} \tag{2.1}$$

with all parameters real (see e.g. [22]). The vacuum state in the IDM is given by:[1]

$$\langle \phi_S \rangle = \frac{1}{\sqrt{2}}\begin{pmatrix} 0 \\ v \end{pmatrix}, \qquad \langle \phi_D \rangle = \frac{1}{\sqrt{2}}\begin{pmatrix} 0 \\ 0 \end{pmatrix}, \quad v = 246 \text{ GeV}. \tag{2.2}$$

The first doublet, ϕ_S, contains the SM-like Higgs boson h with mass M_h equal to

$$M_h^2 = \lambda_1 v^2 = m_{11}^2 = (125 \text{ GeV})^2 . \tag{2.3}$$

The second doublet, ϕ_D, consists of four dark (inert) scalars H, A, $H^\pm$, which do not couple to fermions at the tree-level. Due to an exact D symmetry the lightest neutral scalar H (or A) is stable and can play a role of the DM.[2] The masses of the dark particles read:

$$\begin{aligned} M_{H^\pm}^2 &= \frac{1}{2}\left(\lambda_3 v^2 - m_{22}^2\right), \\ M_A^2 &= M_{H^\pm}^2 + \frac{1}{2}\left(\lambda_4 - \lambda_5\right)v^2, \quad M_H^2 = M_{H^\pm}^2 + \frac{1}{2}\left(\lambda_4 + \lambda_5\right)v^2 . \end{aligned} \tag{2.4}$$

We take H to be the DM candidate and so $M_H < M_A, M_{H^\pm}$ ($\lambda_5 < 0,\ \lambda_4 + \lambda_5 < 0$).

[1] In a 2HDM with the potential V (2.1) different vacua can exist, e.g. a mixed one with $\langle \phi_S \rangle \neq 0$, $\langle \phi_D \rangle \neq 0$ or an inertlike vacuum with $\langle \phi_S \rangle = 0$, $\langle \phi_D \rangle \neq 0$, see [22–25].

[2] Charged DM in the IDM is excluded by the interplay between perturbativity and positivity constraints [22].

JHEP09(2013)055

The properties of the IDM can be described by the parameters of the potential m_{ii}^2 and λ_i or by the masses of the scalar particles and their physical couplings. The parameter $\lambda_{345} = \lambda_3 + \lambda_4 + \lambda_5$ is related to a triple and a quartic coupling between the SM-like Higgs h and the DM candidate H, while λ_3 describes the Higgs particle interaction with charged scalars $H^\pm$. The parameter λ_2 gives the quartic self-couplings of dark particles. Physical parameters are limited by various theoretical and experimental constraints (see e.g. [20, 33–47]). We take the following conditions into account:

Vacuum stability. We require that the potential is bounded from below, which leads to the following constraints [48]:

$$\lambda_1 > 0, \quad \lambda_2 > 0, \quad \lambda_3 + \sqrt{\lambda_1 \lambda_2} > 0, \quad \lambda_{345} + \sqrt{\lambda_1 \lambda_2} > 0 \ \ (\lambda_{345} = \lambda_3 + \lambda_4 + \lambda_5). \quad (2.5)$$

These are tree-level positivity conditions, which ensure the existence of a global minimum. It is known that in the Standard Model the radiative corrections, mainly the top quark contribution, lead to negative values of the Higgs self-coupling, and thus to the instability of the SM vacuum for larger energy scales. The SM vacuum can be metastable, if its lifetime is long enough, i.e. longer than the lifetime of the Universe, see e.g. [49]. An analysis of the stability of the potential in the IDM beyond the tree-level approximation is more complicated and it is beyond the scope of this paper. However, it has been shown in ref. [50] that in the IDM the contributions from four additional scalar states will in general lead to the relaxation of the stability bound, as compared to the SM. This allows the IDM to be valid (i.e. having a stable, and not a metastable vacuum) up to the Planck scale, for a wide portion of the parameter space of the IDM for the currently measured values of the Higgs boson and top quark masses.

Existence of inert vacuum. In the IDM two minima of different symmetry properties can coexist [22–25]. For the state (2.2) to be not just a *local*, but the *global* minimum, the following condition has to be fulfilled [22]:[3]

$$m_{11}^2/\sqrt{\lambda_1} > m_{22}^2/\sqrt{\lambda_2}. \quad (2.6)$$

Perturbative unitarity. Parameters of the potential are constrained by the following bound on the eigenvalues of the high-energy scattering matrix of the scalar sector: $|\Lambda_i| < 8\pi$ [42–44], which leads to the upper limit on the DM quartic self-coupling:

$$\lambda_2^{\max} = 8.38. \quad (2.7)$$

The value of the Higgs boson mass (2.3) and conditions (2.5), (2.6), (2.7) provide the following constraints [44]:

$$\lambda_1 = 0.258, \quad m_{22}^2 \lesssim 9 \cdot 10^4\,\mathrm{GeV}^2, \quad \lambda_3, \lambda_{345} > -\sqrt{\lambda_1 \lambda_2} \geqslant -1.47. \quad (2.8)$$

[3] In principle the IDM allows for tree-level metastability, if the inert minimum is a local one with a lifetime larger than the age of the Universe. In such a case the inertlike minimum would be a true vacuum. However, for the sake of clarity in this work we limit ourselves only to a case in which inert is a global minimum.

JHEP09(2013)055

EWPT. Values of the S and T parameters should lie within 2σ ellipses of the (S,T) plane with the following central values [52]: $S = 0.03 \pm 0.09$, $T = 0.07 \pm 0.08$, with correlation equal to 87%.

LEP limits. The LEP II analysis excludes the region of masses in the IDM where simultaneously [45, 46]:

$$M_H < 80 \text{ GeV}, \ M_A < 100 \text{ GeV and } \delta_A = M_A - M_H > 8 \text{ GeV}. \tag{2.9}$$

For $\delta_A < 8\,\text{GeV}$ the LEP I limit applies [45, 46]:

$$M_H + M_A > M_Z. \tag{2.10}$$

The standard limits for the charged scalar in 2HDM do not apply, as $H^\pm$ has no couplings to fermions. Its mass is indirectly constrained by the studies of supersymmetric models at LEP to be [53]:

$$M_{H^\pm} \gtrsim 70 - 90 \text{ GeV}. \tag{2.11}$$

Relic density constraints. In a big part of the parameter space of the IDM the value of $\Omega_{DM}h^2$ predicted by the IDM is too low, meaning that H does not constitute 100% of DM in the Universe. However, there are three regions of M_H in agreement with $\Omega_{DM}h^2$ (1.1): (i) light DM particles with mass $\lesssim 10$ GeV, (ii) medium DM mass of $40 - 150$ GeV and (iii) heavy DM with mass $\gtrsim 500$ GeV. Proper relic density (1.1) can be obtained by tuning the λ_{345} coupling, and in some cases also by the coannihilation between H and other dark scalars and interference processes with virtual EW gauge bosons [20, 21, 23, 24, 34–40, 54].

3 $R_{\gamma\gamma}$ constraints for the dark scalars

A SM-like Higgs particle was discovered at the LHC in 2012. $R_{\gamma\gamma}$, the ratio of the diphoton decay rate of the observed h to the SM prediction, is sensitive to the "new physics". The current measured values of $R_{\gamma\gamma}$ provided by the ATLAS and the CMS collaborations are respectively [55, 56]:

$$\text{ATLAS}: R_{\gamma\gamma} = 1.65 \pm 0.24(\text{stat})^{+0.25}_{-0.18}(\text{syst}), \tag{3.1}$$

$$\text{CMS}: R_{\gamma\gamma} = 0.79^{+0.28}_{-0.26}. \tag{3.2}$$

Both of them are in 2σ agreement with the SM value $R_{\gamma\gamma} = 1$, however a deviation from that value is still possible and would be an indication of physics beyond the SM.

The ratio $R_{\gamma\gamma}$ in the IDM is given by:

$$R_{\gamma\gamma} := \frac{\sigma(pp \to h \to \gamma\gamma)^{\text{IDM}}}{\sigma(pp \to h \to \gamma\gamma)^{\text{SM}}} \approx \frac{\Gamma(h \to \gamma\gamma)^{\text{IDM}}}{\Gamma(h \to \gamma\gamma)^{\text{SM}}} \frac{\Gamma(h)^{\text{SM}}}{\Gamma(h)^{\text{IDM}}}, \tag{3.3}$$

where $\Gamma(h)^{\text{SM}}$ and $\Gamma(h)^{\text{IDM}}$ are the total decay widths of the Higgs boson in the SM and the IDM respectively, while $\Gamma(h \to \gamma\gamma)^{\text{SM}}$ and $\Gamma(h \to \gamma\gamma)^{\text{IDM}}$ are the respective partial decay widths for the process $h \to \gamma\gamma$. In (3.3) the facts that the main production channel

JHEP09(2013)055

is gluon fusion and that the Higgs particle from the IDM is SM-like, so $\sigma(gg \to h)^{\rm IDM} = \sigma(gg \to h)^{\rm SM}$, were used. In the IDM two sources of deviation from $R_{\gamma\gamma} = 1$ are possible. First is a charged scalar contribution to the partial decay width $\Gamma(h \to \gamma\gamma)^{\rm IDM}$ [20, 57–60]:

$$\Gamma(h \to \gamma\gamma)^{\rm IDM} = \frac{G_F \alpha^2 M_h^3}{128\sqrt{2}\pi^3} \left| \underbrace{\frac{4}{3} A_{1/2}\left(\frac{4M_t^2}{M_h^2}\right) + A_1\left(\frac{4M_W^2}{M_h^2}\right)}_{\mathcal{M}^{\rm SM}} + \underbrace{\frac{\lambda_3 v^2}{2M_{H^\pm}^2} A_0\left(\frac{4M_{H^\pm}^2}{M_h^2}\right)}_{\delta\mathcal{M}^{\rm IDM}} \right|^2 , \tag{3.4}$$

where $\mathcal{M}^{\rm SM}$ is the SM amplitude and $\delta\mathcal{M}^{\rm IDM}$ is the $H^\pm$ contribution.[4] The interference between $\mathcal{M}^{\rm SM}$ and $\delta\mathcal{M}^{\rm IDM}$ can be either constructive or destructive, leading to an increase or a decrease of the decay rate (3.4).

The second source of modifications of $R_{\gamma\gamma}$ are the possible invisible decays $h \to HH$ and $h \to AA$, which can strongly augment the total decay width $\Gamma^{\rm IDM}(h)$ with respect to the SM case. Partial widths for these decays are given by:

$$\Gamma(h \to HH) = \frac{\lambda_{345}^2 v^2}{32\pi M_h} \sqrt{1 - \frac{4M_H^2}{M_h^2}} , \tag{3.5}$$

with M_H exchanged to M_A and λ_{345} to λ_{345}^- ($\lambda_{345}^- = \lambda_3 + \lambda_4 - \lambda_5$), for the $h \to AA$ decay. Using eq. (2.4) one can reexpress the couplings λ_3 and λ_{345}^- in terms of M_H, M_A, $M_{H^\pm}$ and λ_{345}, and so from eq. (3.4) and (3.5) $R_{\gamma\gamma}$ depends only on the masses of the dark scalars and λ_{345}.

For $M_H > M_h/2$ (and $M_A > M_h/2$) the invisible channels are closed, and $R_{\gamma\gamma} > 1$ is possible, with the maximal value of $R_{\gamma\gamma}$ equal to 3.69 for $M_H = M_{H^\pm} = 70\,\text{GeV}$.

If $M_H < M_h/2$ then the $h \to HH$ invisible channel is open and it is not possible to obtain $R_{\gamma\gamma} > 1$, as shown in [60, 61]. If an enhancement (3.1) in the diphoton channel is confirmed, this DM mass region is already excluded. However, if the final value of $R_{\gamma\gamma}$ is below 1, as suggested by the CMS data (3.2), then it limits the parameters of the IDM on the basis of the following reasoning. For any given values of the dark scalars' masses $R_{\gamma\gamma}$ is a function of one parameter: λ_{345}, the behaviour of which is presented in figure 1 for $M_H = 55\,\text{GeV}$, $M_A = 60\,\text{GeV}$, $M_{H^\pm} = 120\,\text{GeV}$ (the same shape of the curve is preserved for different values of masses). It can be observed, that setting a lower bound on $R_{\gamma\gamma}$ leads to upper and lower bounds on λ_{345}. We will explore these bounds, as functions of M_H and δ_A in sections 3.1 and 3.2 for three cases that are in 1σ region of the CMS value: $R_{\gamma\gamma} > 0.7, 0.8, 0.9$, respectively.

3.1 HH, AA decay channels open

If both $M_H, M_A < M_h/2$ then the LEP constraint (2.9) enforces $\delta_A < 8\,\text{GeV}$ and so eq. (2.10) limits the allowed values of the DM particle mass $M_H > (M_Z - 8\,\text{GeV})/2 \approx 41\,\text{GeV}$. In this region, the invisible decay channels have stronger influence on the value of $R_{\gamma\gamma}$ than the contribution from the charged scalar loop [61], and so the exact value of $M_{H^\pm}$ influences the results less than the other scalar masses. In the following examples we

[4] The definition of the functions A_i can be found in refs. [57, 58].

JHEP09(2013)055

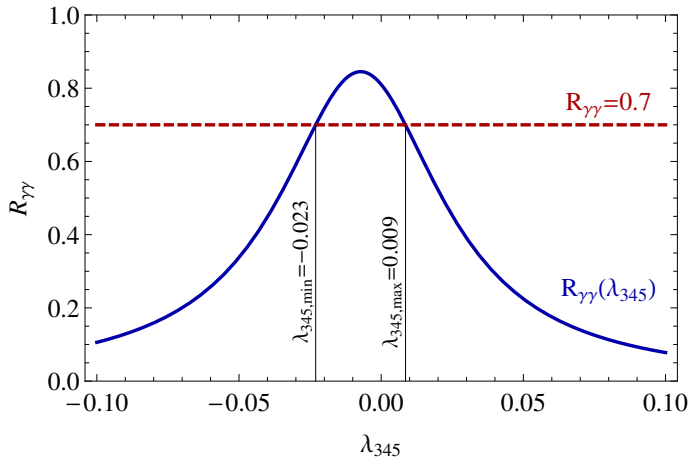

Figure 1. $R_{\gamma\gamma}$ as a function of λ_{345} for the following masses of dark scalars: $M_H = 55\,\text{GeV}$, $M_A = 60\,\text{GeV}$, $M_{H^\pm} = 120\,\text{GeV}$. The bounds on λ_{345} coming from the requirement that $R_{\gamma\gamma} > 0.7$ are shown.

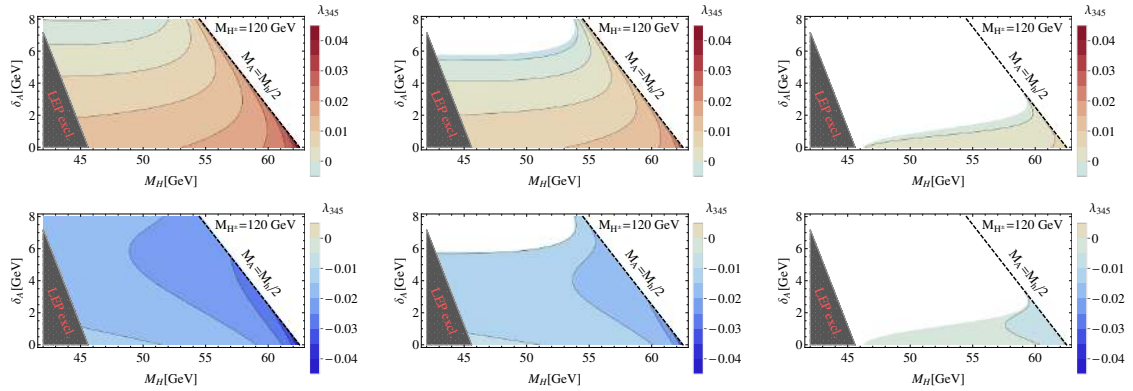

(a) $R_{\gamma\gamma} > 0.7$ (b) $R_{\gamma\gamma} > 0.8$ (c) $R_{\gamma\gamma} > 0.9$

Figure 2. Upper (upper panel) and lower (lower panel) limits on λ_{345} coming from the requirement that (a) $R_{\gamma\gamma} > 0.7$, (b) $R_{\gamma\gamma} > 0.8$, (c) $R_{\gamma\gamma} > 0.9$, expressed as functions of M_H and δ_A for the case when the $h \to HH$, AA channels are open ($M_H, M_A < M_h/2$). $M_{H^\pm}$ is set to 120 GeV. The lower left corner is excluded by LEP.

use $M_{H^\pm} = 120\,\text{GeV}$, which is a good benchmark value of the charged scalar mass in the DM analysis for the low and medium DM mass regions, discussed later in section 4. Due to the dependence of the partial width $\Gamma(h \to AA)$ on $|\lambda_{345}^-|$ the obtained lower and upper bounds are not symmetric with respect to $\lambda_{345} = 0$.

Diphoton rate constraints. Figure 2(a) shows the upper and lower limits for the λ_{345} coupling if $R_{\gamma\gamma} > 0.7$. The allowed values of λ_{345} are small, typically between $(-0.04, 0.04)$, depending on the difference between masses of H and A. In general, for $R_{\gamma\gamma} > 0.8$ the allowed values of λ_{345} are smaller than for $R_{\gamma\gamma} > 0.7$. Also, region of larger δ_A is excluded (figure 2(b)). In contrast to the previous cases condition $R_{\gamma\gamma} > 0.9$ strongly limits the

JHEP09(2013)055

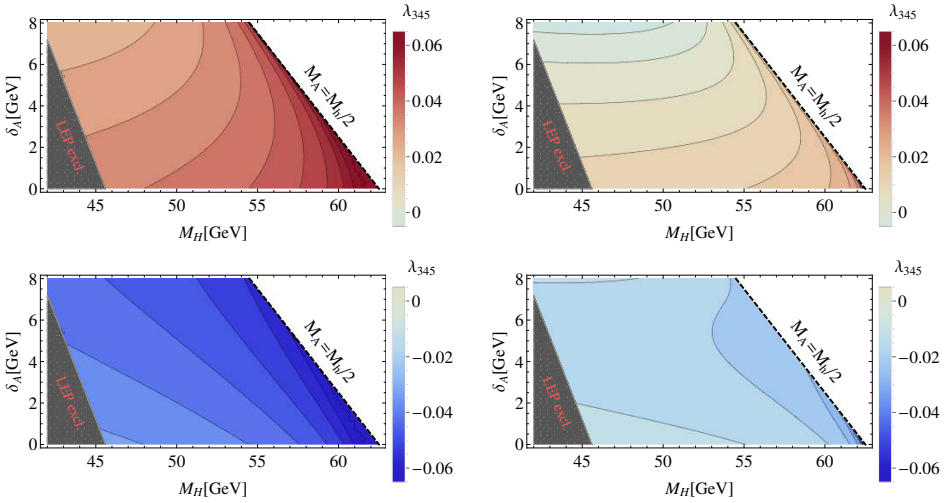

(a) $\mathrm{Br}(h \to \mathrm{inv}) < 65\%$ (b) $\mathrm{Br}(h \to \mathrm{inv}) < 20\%$

Figure 3. Upper (upper panel) and lower (lower panel) limits on λ_{345} coming from the requirement that (a) $\mathrm{Br}(h \to \mathrm{inv}) < 65\%$, (b) $\mathrm{Br}(h \to \mathrm{inv}) < 20\%$ expressed as functions of M_H and δ_A for the case when the $h \to HH$, AA channels are open. The lower left corner is excluded by LEP.

allowed parameter space of the IDM, as shown in figure 2(c), where a large portion of the parameter space is excluded. The allowed A, H mass difference is $\delta_A \lesssim 2\,\mathrm{GeV}$, and values of λ_{345} are smaller than in the previous cases. Requesting larger $R_{\gamma\gamma}$ leads to the exclusion of the whole region of masses, apart from $M_H \approx M_A \approx M_h/2$.

Br($h \to$ inv). In principle, while discussing the $M_H < M_h/2$ region, one should also include the constraints from existing LHC data on the invisible channels branching ratio [50, 62]. However, constraints on λ_{345} obtained by requesting $\mathrm{Br}(h \to \mathrm{inv}) < 65\,\%$ [55] are up to 50% weaker than those coming from $R_{\gamma\gamma}$, compare figure 2 and figure 3(a). The limits from the invisible branching ratio start to be comparative with the $R_{\gamma\gamma}$ constraints when $\mathrm{Br}(h \to \mathrm{inv}) < 20\,\%$, as estimated in [63, 64].

3.2 *AA* decay channel closed

When the AA decay channel is closed, a very light DM particle can exist. Of course, if the AA channel is closed the values of $R_{\gamma\gamma}$ do not depend on the value of M_A, while the charged scalar contribution becomes more relevant. A clear dependence on the $H^\pm$ mass appears especially for $M_{H^\pm} \lesssim 120\,\mathrm{GeV}$. Figure 4 shows the limits on λ_{345} coupling that allow values of $R_{\gamma\gamma}$ higher than 0.7, 0.8 and 0.9 for $M_{H^\pm} = 70$, 120 and 500 GeV, respectively. Larger value of $R_{\gamma\gamma}$ leads to smaller allowed values of λ_{345}. In the case of $R_{\gamma\gamma} > 0.9$ a large region of DM masses is excluded, as it is not possible to obtain the requested value of $R_{\gamma\gamma}$ for any value of λ_{345}.

If $R_{\gamma\gamma} > 0.7$ then an exact value of $M_{H^\pm}$ is not crucial for the obtained limits on λ_{345}, and allowed values of $|\lambda_{345}|$ are of the order of 0.02. For $R_{\gamma\gamma} > 0.8$ the obtained bounds

JHEP09(2013)055

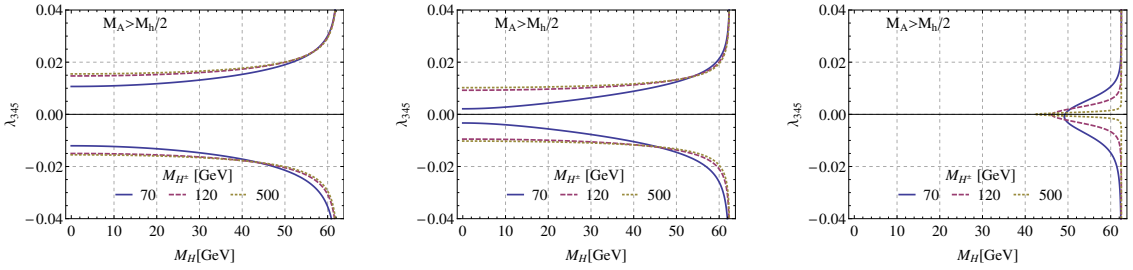

(a) $R_{\gamma\gamma} > 0.7$ (b) $R_{\gamma\gamma} > 0.8$ (c) $R_{\gamma\gamma} > 0.9$

Figure 4. Upper and lower limits on λ_{345} coming from the requirement that (a) $R_{\gamma\gamma} > 0.7$, (b) $R_{\gamma\gamma} > 0.8$, (c) $R_{\gamma\gamma} > 0.9$, expressed as functions of M_H, for the case when the $h \to AA$ channel is closed. Three values of $M_{H^\pm}$ are considered $M_{H^\pm} = 70\,\text{GeV}$, $M_{H^\pm} = 120\,\text{GeV}$, $M_{H^\pm} = 500\,\text{GeV}$.

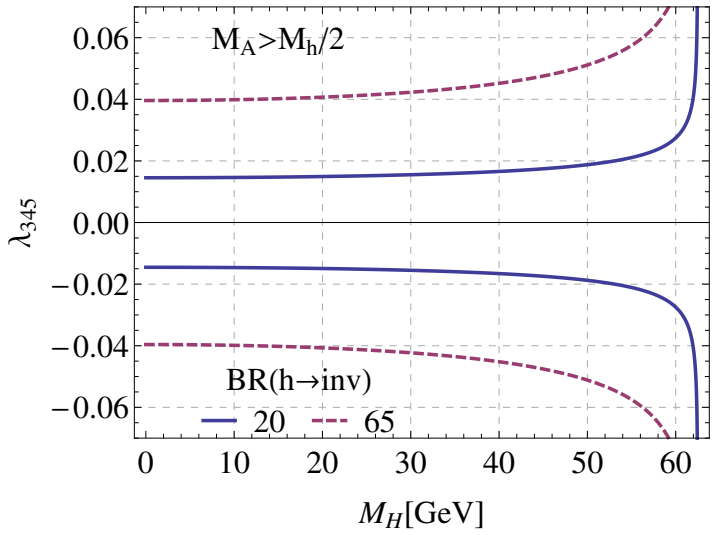

Figure 5. Upper and lower limits on λ_{345} coming from the bounds on the branching ratio: $\text{Br}(h \to \text{inv}) < 65\%$ (dashed line) and $\text{Br}(h \to \text{inv}) < 20\%$ (solid line), expressed as a function of M_H, for the case when the $h \to AA$ channel is closed.

are clearly different for $M_{H^\pm} = 70\,\text{GeV}$ and $120\,\text{GeV}$. Smaller $H^\pm$ mass leads to stronger limits, requiring $|\lambda_{345}| \sim 0.005$, while larger masses of $H^\pm$ allow $|\lambda_{345}| \sim 0.015$.

Condition $R_{\gamma\gamma} > 0.9$ limits the IDM parameter space strongly. It is not possible to have $R_{\gamma\gamma} > 0.9$ if $M_H \lesssim 45\,\text{GeV}$. For the larger masses only relatively small values of λ_{345} (below 0.02) are allowed. It is interesting to note, that in this case not smaller, but larger $M_{H^\pm}$ leads to more stringent limits on λ_{345}.

Br($h \to$ inv). Similarly to the $M_A < M_h/2$ case, the constraint from the invisible decay branching ratio $\text{Br}(h \to \text{inv}) < 65\%$ does not further limit the values of λ_{345}, compare figure 4 and figure 5. Bounds obtained from $\text{Br}(h \to \text{inv}) < 20\%$ are competitive with those coming from $R_{\gamma\gamma}$.

JHEP09(2013)055

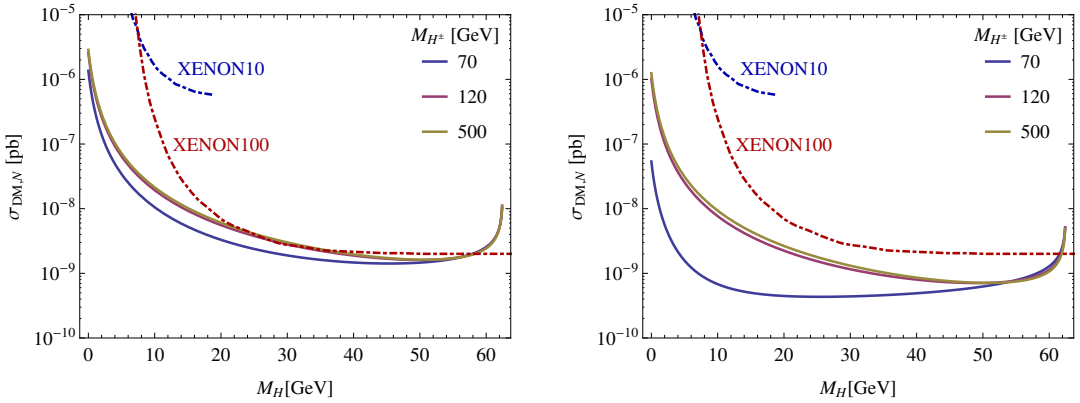

(a) $R_{\gamma\gamma} > 0.7$ (b) $R_{\gamma\gamma} > 0.8$

Figure 6. Upper limit on $\sigma_{\mathrm{DM},N}$ (3.6) with $f_N = 0.326$ coming from the requirement that (a) $R_{\gamma\gamma} > 0.7$, (b) $R_{\gamma\gamma} > 0.8$, expressed as a function of M_H, for the case when the $h \to AA$ channel is closed. Three values of $M_{H^\pm}$ are considered: $M_{H^\pm} = 70\,\mathrm{GeV}$, $M_{H^\pm} = 120\,\mathrm{GeV}$, $M_{H^\pm} = 500\,\mathrm{GeV}$. For comparison also the upper bounds set by XENON10 and XENON100 are shown.

DM-nucleon cross section. In the IDM the DM-nucleon scattering cross-section $\sigma_{DM,N}$ is given by:

$$\sigma_{\mathrm{DM,N}} = \frac{\lambda_{345}^2}{4\pi M_h^4} \frac{m_N^4}{(m_N + M_H)^2} f_N^2 \,, \tag{3.6}$$

where we take $M_h = 125\,\mathrm{GeV}$, $m_N = 0.939\,\mathrm{GeV}$ and $f_N = 0.326$ as the universal Higgs-nucleon coupling.[5] Value of the λ_{345} coupling is essential for the value of $\sigma_{DM,N}$ in the IDM and so we translate the limits for λ_{345} obtained from $R_{\gamma\gamma}$ measurements to $(M_H, \sigma_{DM,N})$ plane, used in direct detection experiments.

Exclusion bounds for cases $R_{\gamma\gamma} > 0.7, 0.8$ are shown in figure 6, along with the XENON10/100 limits [7]. If H should constitute 100% of DM in the Universe, then the limits set by $R_{\gamma\gamma}$ measurements are much stronger than the ones provided by XENON10/100 experiments for $M_H \lesssim 20\,\mathrm{GeV}$. Even for $R_{\gamma\gamma} > 0.7$ it provides stronger or comparable limits for $\sigma_{DM,N}$ for $M_H \lesssim 60\,\mathrm{GeV}$.

3.3 Invisible decay channels closed

If $M_H > M_h/2$, and consequently $M_A > M_h/2$, the invisible channels are closed and the only modification to $R_{\gamma\gamma}$ comes from the charged scalar loop (3.4), so the most important parameters are $M_{H^\pm}$ and λ_3 (or equivalently m_{22}^2). The contribution from the SM ($\mathcal{M}^{\mathrm{SM}}$) is real and negative and $\delta\mathcal{M}^{\mathrm{IDM}}$ is also real with sign correlated with the sign of λ_3. Enhancement in $R_{\gamma\gamma}$ is possible when $\lambda_3 < 0$ [60, 61, 66, 67], with the maximal value of $R_{\gamma\gamma}$ approached for $\lambda_3 = -1.47$, i.e. the smallest value of this parameter allowed by model constraints (2.8).

The contribution to the amplitude from the charged scalar loop ($\delta\mathcal{M}^{\mathrm{IDM}}$) is a decreasing function of $M_{H^\pm}$ so in general the larger $R_{\gamma\gamma}$ is, the smaller $M_{H^\pm}$ should be. For example, $R_{\gamma\gamma} > 1.2$ gives $70\,\mathrm{GeV} < M_{H^\pm} < 154\,\mathrm{GeV}$ [61].

[5] There is no agreement on the value of the f_N coupling and various estimations exist in the literature. Here we consider the middle value of $0.14 < f_N < 0.66$ [65], and comment on the other possible values later in the text (see also discussion in [50]).

JHEP09(2013)055

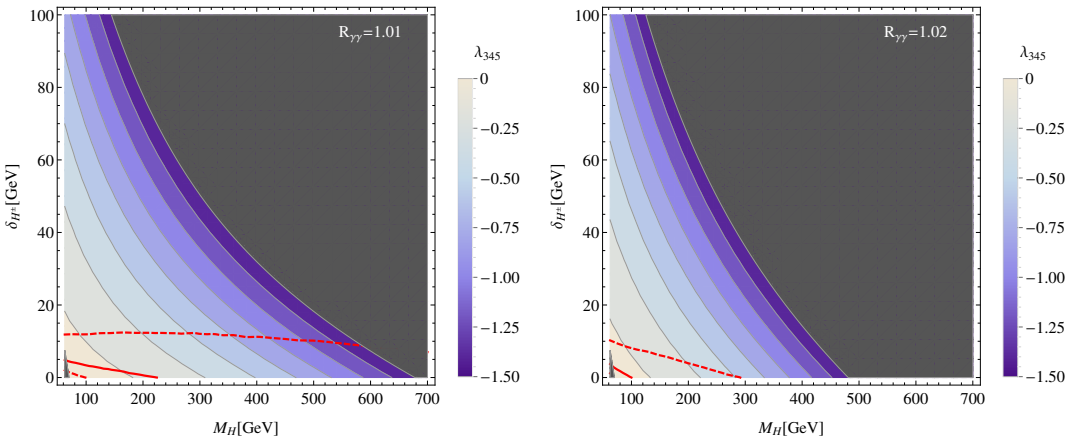

(a) $R_{\gamma\gamma} = 1.01$ (b) $R_{\gamma\gamma} = 1.02$

Figure 7. Allowed regions in $(M_H,\ \delta_{H^\pm})$ plane for two values of $R_{\gamma\gamma}$: 1.01 (left panel), 1.02 (right panel). Dark grey region is excluded due to LEP bounds (left lower corner) and the vacuum stability/unitarity constraints (2.8) (right upper corner). Red lines show bounds from XENON100 (solid for $f_N = 0.326$, dashed for $f_N = 0.14$ and $f_N = 0.66$) — region above this line is excluded, if we assume that the dark scalar H constitutes all dark matter relic density.

Since for invisible channels closed $R_{\gamma\gamma}$ depends only on $M_{H^\pm}$ and λ_3 (or m_{22}^2), fixing $R_{\gamma\gamma}$ and $M_{H^\pm}$ sets the value of m_{22}^2. For fixed m_{22}^2, M_H depends only on λ_{345}, eq. (2.4). Thus, we can study the correlation between $M_{H^\pm}$, M_H and λ_{345} for different values of $R_{\gamma\gamma}$. Figure 7 shows the ranges of λ_{345} in the $(M_{H^\pm}, \delta_{H^\pm})$ plane for two values of $R_{\gamma\gamma}$ close to 1, $R_{\gamma\gamma} = 1.01$ and 1.02. One can see that even a small deviation from $R_{\gamma\gamma} = 1$ requires a relatively large λ_{345}, if the mass difference $\delta_{H^\pm}$ is of the order $(50 - 100)\,\mathrm{GeV}$. Small values of $|\lambda_{345}|$ are preferred if the mass difference is small.

Unitarity and positivity limits on λ_3 and λ_{345}, eq. (2.8), constrain the allowed value of $M_{H^\pm}$ (and thus also the mass of H) for a given value of $R_{\gamma\gamma}$. For $R_{\gamma\gamma}^{\max} = 1.01$ masses of $M_{H^\pm} \gtrsim 700\,\mathrm{GeV}$ are excluded, and if $R_{\gamma\gamma}^{\max} = 1.02$ this bound is stronger, forbidding $M_{H^\pm} \gtrsim 480\,\mathrm{GeV}$ (figure 7).

The blue curve in figure 8 shows the maximal value of $R_{\gamma\gamma}$, which is obtained for maximally allowed negative value of $\lambda_3 = -1.47$, as a function of $M_{H^\pm}$. In general, as previous studies have shown, the very heavy mass region is consistent with very small deviations from $R_{\gamma\gamma} = 1$, but substantial enhancement of $R_{\gamma\gamma}$ suggested by the central value measured by ATLAS (3.1) cannot be reconciled with this region of masses.

$R_{\gamma\gamma} < 1$ is possible if the invisible channels are closed and $\lambda_3 > 0$. Requiring that $R_{\gamma\gamma}$ is bounded from above one can also limit the allowed parameter space. For example, if $R_{\gamma\gamma} < 0.8$ and invisible channels are closed, then $M_H < 200\,\mathrm{GeV}$ [61].

Comparison with XENON100 results. If the dark scalars H constitute 100% of DM in the Universe, then the $\sigma_{DM,N}$ measurements done by the direct detection experiments bound the λ_{345} parameter, which is also constrained by the $R_{\gamma\gamma}$ value (figure 7). For given scalar masses one can test the compability between the two limits, and figure 7 shows that

JHEP09(2013)055

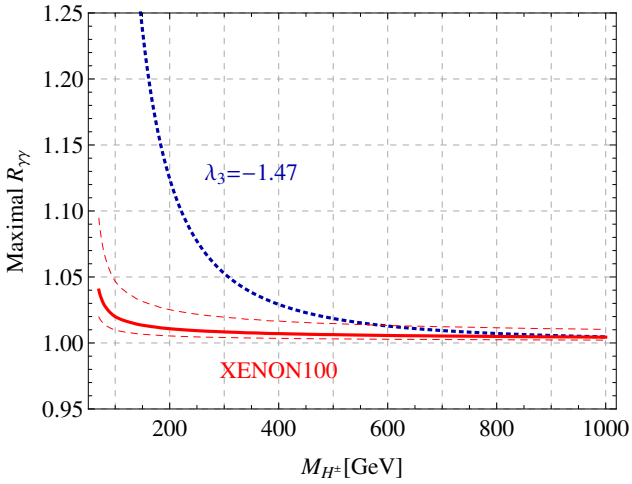

Figure 8. Blue (thick dashed) curve: the maximal value of $R_{\gamma\gamma}$, allowed by the condition $\lambda_{345} > -1.47$ (eq. (2.8)) as a function of $M_{H^\pm}$. Red lines (solid/thin dashed): the maximal value of $R_{\gamma\gamma}$, allowed by the XENON100 constraints on λ_{345} (derived using the assumption that H constitutes 100% of DM) as a function of $M_{H^\pm}$, for $M_{H^\pm} = M_H$. Solid red line corresponds to the bounds obtained for $f_N = 0.326$ as in [68], while upper dashed for $f_N = 0.14$ and lower dashed for $f_N = 0.66$.

$R_{\gamma\gamma} > 1$ and agreement with XENON100 need almost degenerated masses of H and $H^\pm$. If $\delta_{H^\pm}$ is larger then $R_{\gamma\gamma}$ requires larger λ_{345}, and that violates the XENON100 bounds (figure 7).

For a given value of M_H one can find maximal negative value of λ_{345} allowed by XENON100 experiment. Assuming that M_H and $M_{H^\pm}$ are degenerate allows to compute maximal allowed value of $R_{\gamma\gamma}$. The dependence of maximal $R_{\gamma\gamma}$ on $M_{H^\pm} = M_H$ for different values of f_N is shown in figure 8 (red curves). For $M_H \approx M_{H^\pm} = 70$ GeV, the $R_{\gamma\gamma}$ is bounded by (1.09, 1.04, 1.02) for $f_N = (0.14, 0.326, 0.66)$ respectively. Thus it is not possible to have $R_{\gamma\gamma} > 1.09$ in agreement with XENON100, unless the dark scalar H constitutes only a part of the dark matter relic density.

4 Combining $R_{\gamma\gamma}$ and relic density constraints on DM

In this section we compare the limits on the λ_{345} parameter obtained from $R_{\gamma\gamma}$ in the previous section with those coming from the requirement that the DM relic density is in agreement with the WMAP measurements (1.1). We use the micrOMEGAs package [69] to calculate $\Omega_{DM}h^2$ for chosen values of DM masses. We demand that the obtained value lies in the 3σ WMAP limit:

$$0.1018 < \Omega_{DM}h^2 < 0.1234\,. \tag{4.1}$$

If this condition is fulfilled, then H constitutes 100% of DM in the Universe. Values of $\Omega_H h^2 > 0.1234$ are excluded, while $\Omega_H h^2 < 0.1018$ are still allowed if H is a subdominant DM candidate.

JHEP09(2013)055

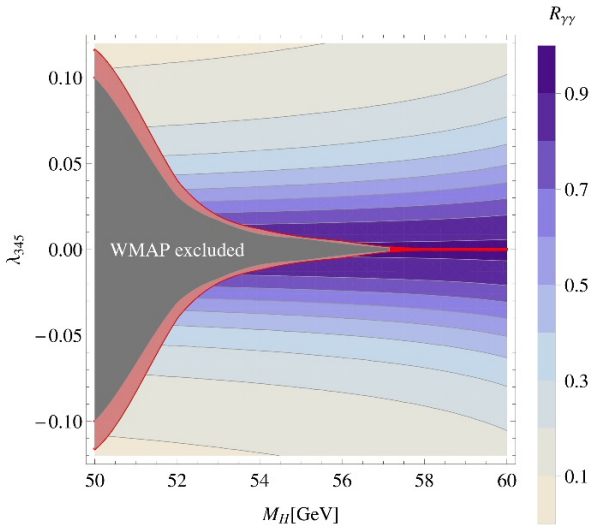

Figure 9. Comparison of the values of $R_{\gamma\gamma}$ and region allowed by the relic density measurements for the middle DM mass region with HH invisible channel open and $M_A = M_{H^\pm} = 120\,\text{GeV}$. Red bound: region in agreement with WMAP (4.1). Grey area: excluded by WMAP. $R_{\gamma\gamma} > 0.7$ limits the allowed values of masses to $M_H > 53\,\text{GeV}$.

4.1 Low DM mass

In the IDM the low DM mass region corresponds to the masses of H below 10 GeV, while the other dark scalars are heavier, $M_A \approx M_{H^+} \approx 100\,\text{GeV}$. In this region the main annihilation channel is $HH \to h \to \bar{b}b$ and to have the proper relic density, the HHh coupling (λ_{345}) has to be large, above $\mathcal{O}(0.1)$. For example, for CDMS-II favoured mass $M = 8.6\,\text{GeV}$ [5] one gets relic density in agreement with bound (4.1) for $|\lambda_{345}| = (0.35 - 0.41)$, while $|\lambda_{345}| \lesssim 0.35$ are excluded.

In the low mass region the invisible channel $h \to HH$ is open, meaning that $R_{\gamma\gamma} > 1$ is not possible, so we can conclude that $R_{\gamma\gamma} > 1$ (3.1) excludes the low DM mass region in the IDM. If $R_{\gamma\gamma} < 1$, as suggested by the CMS data (3.2), the low DM mass could be in principle allowed. However, our results, described in the previous section, show, that it is not possible, as the coupling allowed by $R_{\gamma\gamma}$, i.e. $|\lambda_{345}| \sim 0.02$, is of an order of magnitude smaller than needed for $\Omega_{DM}h^2$. So we can conclude that the low DM mass region cannot be accommodated in the IDM with recent LHC results, irrespective of whether H is the only, or just a subdominant, DM candidate.

4.2 Medium DM mass

Invisible decay channels open. Let us first consider the case with AA invisible channel closed, where we chose $M_A = M_{H^\pm} = 120\,\text{GeV}$. In this case the main annihilation channels are $HH \to h \to \bar{f}f$, when the HHh coupling is large enough and $HH \to W^+W^-$, when the HHh coupling is suppressed, typically leading to $\Omega_{DM}h^2$ above the WMAP limit. Lower values of M_H require rather large λ_{345} — in this sense this region resembles the low DM mass region. As M_H grows towards $M_H = M_h/2$, the value of λ_{345} required to obtain

JHEP09(2013)055

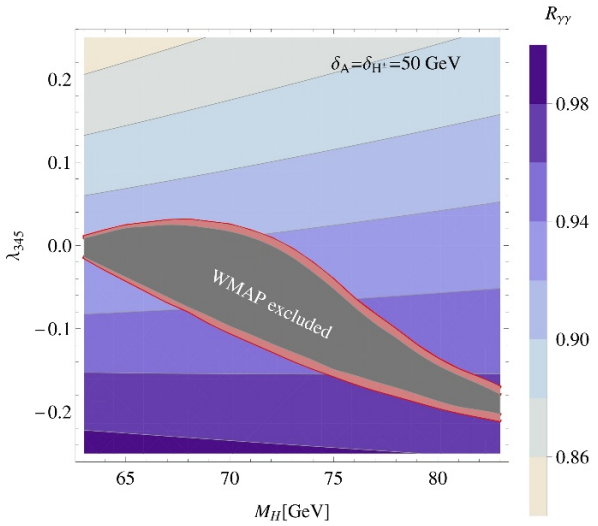

Figure 10. Comparison of the values of $R_{\gamma\gamma}$ and region allowed by the relic density measurements for the middle DM mass region with HH invisible channel closed and $\delta_A = \delta_{H^\pm} = 50\,\mathrm{GeV}$. Red bound: region in agreement with WMAP (4.1). Grey area: excluded by WMAP. $R_{\gamma\gamma} > 1$ is not possible, unless H is a subdominant DM candidate.

the proper relic density gets smaller, leading eventually to the $\Omega_{DM}h^2$ below WMAP limit, apart from extremely tunned and small values of λ_{345}.

These results are presented in figure 9, where the WMAP-allowed range of $\Omega_{DM}h^2$ is denoted by the red bound. Grey excluded region between the WMAP bounds corresponds to $\Omega_{DM}h^2$ too large, leading to the overclosing of the Universe. If we consider H as a subdominant DM candidate with $\Omega_H h^2 < \Omega_{DM}h^2$ then also the regions below and above red bounds in figure 9 are allowed. This usually corresponds to the larger values of λ_{345}. It can be clearly seen that for a large portion of the parameter space limits for λ_{345} from $R_{\gamma\gamma}$, even for the least stringent case $R_{\gamma\gamma} > 0.7$, cannot be reconciled with the WMAP-allowed region.

Invisible decay channels closed. In this analysis we choose $\delta_{H^\pm} = \delta_A = 50\,\mathrm{GeV}$ in agreement with the set of constraints (2.9) and M_H varying between $M_h/2$ and $83\,\mathrm{GeV}$. The main annihilation channels are as in the previous case, with the gauge channels getting more important as the mass of the DM particle grows. This, and the presence of the three body final states with virtual $W^\pm$, are the main reason why the WMAP-allowed region (the red bound) presented in figure 10 is not symmetric around zero, eventually leaving no positive values of λ_{345} allowed. The absolute values of λ_{345} that lead to the proper relic density are in general larger than in the case of $M_H < M_h/2$.

Figure 10 presents the values of $R_{\gamma\gamma}$ for chosen masses and couplings compared to the WMAP-allowed/excluded region. It can be seen that this region is consistent with $R_{\gamma\gamma} < 1$. It is in agreement with results obtained before (figure 7), as mass difference $\delta_{H^\pm} = 50\,\mathrm{GeV}$ and $R_{\gamma\gamma} > 1$ requires $\lambda_{345} \lesssim -0.3$, a value smaller than the one obtained from the relic density limits.

JHEP09(2013)055

We can conclude, that $R_{\gamma\gamma} > 1$ and relic density constraints (4.1) cannot be fulfilled for the middle DM mass region. If the IDM is the source of all DM in the Universe and $M_H \approx (63 - 83)\,\mathrm{GeV}$ then the maximal value of $R_{\gamma\gamma}$ is around 0.98. A subdominant DM candidate, which corresponds to larger λ_{345}, is consistent with $R_{\gamma\gamma} > 1$.

Comparison with the indirect detection limits. The current best limits on DM annihilation into $b\bar{b}$, which is the main annihilation channel for low and medium DM masses in the IDM, come from the measurements of secondary photons from Mikly Way dwarf galaxies and the Galactic Centre region by the Fermi-LAT satellite [70, 71].[6] They exclude the generic WIMP candidates that annihilate mainly into $b\bar{b}$ and reproduce the observed $\Omega_{DM}h^2$ for $M_{DM} \lesssim 25\,\mathrm{GeV}$ [70]. Independent analyses give slightly stronger limits, excluding generic WIMPs with M_{DM} less than 40 GeV [73, 74]. Observations of γ line signals give no further constraints for standard WIMP models [11]. Indirect detections exclusions are in general weaker than those provided by XENON10/XENON100 experiments and can be comparable or stronger only in the low mass regime, where the controversies from the direct detection are the strongest. The combined $\Omega_{DM}h^2$ and $R_{\gamma\gamma}$ analysis, performed here, excludes masses of DM in the IDM below 53 GeV if $R_{\gamma\gamma} > 0.7$ and thus gives stronger limits on the allowed values of masses in the IDM than those currently obtained from the indirect detection experiments.

5 Summary

The IDM is a simple extension of the Standard Model that can provide a scalar DM candidate. This candidate is consistent with the WMAP results on the DM relic density and in three regions of masses it can explain 100 % of the DM in the Universe. In a large part of the parameter space it can also be considered as a subdominant DM candidate. Measurements of the diphoton ratio, $R_{\gamma\gamma}$, recently done by the ATLAS and the CMS experiments at the LHC, set strong limits on masses of the DM and other dark scalars, as well as the self-couplings, especially λ_{345}. In this paper we discuss the obtained constraints for various possible values of $R_{\gamma\gamma}$, that are in agreement with the recent LHC measurements, and combine them with WMAP constraints.

The main results of the present paper are as follows:

- If invisible Higgs decays channels are open ($M_H < M_h/2$) then $R_{\gamma\gamma}$ measurements can constrain the maximal value of $|\lambda_{345}|$. This sets strong limits especially on the low DM mass region in the IDM. Values of $|\lambda_{345}|$ that lead to the proper relic density in the 3σ WMAP range $0.1018 < \Omega_{DM}h^2 < 0.1234$, are an order of magnitude larger than the ones allowed by assuming that $R_{\gamma\gamma} > 0.7$. We conclude that we can exclude the low DM mass region in the IDM, i.e. $M_H \lesssim 10\,\mathrm{GeV}$.

- $R_{\gamma\gamma}$ also provides strong limits for larger values of M_H. First, demanding that $R_{\gamma\gamma} > 0.9$ leaves only a small part of the parameter space allowed, excluding the region $M_A - M_H \gtrsim 2\,\mathrm{GeV}$ if both invisible decay channels are open or $M_H \lesssim 43\,\mathrm{GeV}$

[6] AMS-02 results provide weaker constraints on Dark Matter annihilation into $b\bar{b}$ [72].

JHEP09(2013)055

if the AA channel is closed. Second, comparing $R_{\gamma\gamma}$ limits with the WMAP allowed region, we found that masses $M_H \lesssim 53\,\text{GeV}$, which require larger values of λ_{345} to be in agreement with WMAP, cannot be reconciled with $R_{\gamma\gamma} > 0.7$.

- $R_{\gamma\gamma}$ sets limits on the DM-nucleon scattering cross-section in the low and medium DM mass region, which are stronger or comparable with the results obtained both by the XENON100 and Fermi-LAT experiments.

- If the invisible decay channels are closed, then $R_{\gamma\gamma} > 1$ is possible. This however leads to the constraints on masses and couplings. In general, $R_{\gamma\gamma} > 1$ favours the degenerated H and $H^{\pm}$. When the mass difference is large, $\delta_{H^{\pm}} \approx (50 - 100)\,\text{GeV}$, then the required values of $|\lambda_{345}|$ that provide $R_{\gamma\gamma} > 1$ are bigger than those allowed by WMAP measurements. We conclude it is not possible to have all DM in the Universe explained by the IDM (in the low and medium DM mass regime) and $R_{\gamma\gamma} > 1$. If $R_{\gamma\gamma} > 1$ then H may be a subdominant DM candidate. If $R_{\gamma\gamma} < 1$ then $M_H \approx (63 - 80)\,\text{GeV}$ can explain 100% of DM in the Universe.

Acknowledgments

We thank Sabine Kraml and Sara Rydbeck for comments and suggestions. This work was supported in part by the grant NCN OPUS 2012/05/B/ST2/03306 (2012-2016).

References

[1] J. Beringer et al., *Review of particle physics*, *Phys. Rev.* **D 86** (2012) 010001 [INSPIRE].

[2] DAMA collaboration, R. Bernabei et al., *First results from DAMA/LIBRA and the combined results with DAMA/NaI*, *Eur. Phys. J.* **C 56** (2008) 333 [arXiv:0804.2741] [INSPIRE].

[3] CoGeNT collaboration, C. Aalseth et al., *Results from a search for light-mass dark matter with a p-type point contact germanium detector*, *Phys. Rev. Lett.* **106** (2011) 131301 [arXiv:1002.4703] [INSPIRE].

[4] C. Aalseth et al., *Search for an annual modulation in a p-type point contact germanium dark matter detector*, *Phys. Rev. Lett.* **107** (2011) 141301 [arXiv:1106.0650] [INSPIRE].

[5] CDMS collaboration, R. Agnese et al., *Dark matter search results using the silicon detectors of CDMS II*, *Phys. Rev. Lett.* (2013) [arXiv:1304.4279] [INSPIRE].

[6] G. Angloher et al., *Results from 730 kg days of the CRESST-II dark matter search*, *Eur. Phys. J.* **C 72** (2012) 1971 [arXiv:1109.0702] [INSPIRE].

[7] XENON100 collaboration, E. Aprile et al., *Dark matter results from* 225 *live days of XENON100 data*, *Phys. Rev. Lett.* **109** (2012) 181301 [arXiv:1207.5988] [INSPIRE].

JHEP09(2013)055

[8] T. Bringmann, X. Huang, A. Ibarra, S. Vogl and C. Weniger, *Fermi LAT search for internal bremsstrahlung signatures from dark matter annihilation*, *JCAP* **07** (2012) 054 [arXiv:1203.1312] [INSPIRE].

[9] C. Weniger, *A tentative γ-ray line from dark matter annihilation at the Fermi Large Area Telescope*, *JCAP* **08** (2012) 007 [arXiv:1204.2797] [INSPIRE].

[10] FERMI-LAT collaboration, *Search for γ-ray spectral lines with the Fermi Large Area Telescope and dark matter implications*, arXiv:1305.5597 [INSPIRE].

[11] T. Bringmann and C. Weniger, *Gamma ray signals from dark matter: concepts, status and prospects*, *Phys. Dark Univ.* **1** (2012) 194 [arXiv:1208.5481] [INSPIRE].

[12] L. Bergstrom, *Dark matter evidence, particle physics candidates and detection methods*, *Annalen Phys.* **524** (2012) 479 [arXiv:1205.4882] [INSPIRE].

[13] J. Collar and D. McKinsey, *Comments on 'First dark matter results from the XENON100 experiment'*, arXiv:1005.0838 [INSPIRE].

[14] XENON100 collaboration, *Reply to the comments on the XENON100 first dark matter results*, arXiv:1005.2615 [INSPIRE].

[15] J. Collar and D. McKinsey, *Reply to arXiv:1005:2615*, arXiv:1005.3723 [INSPIRE].

[16] J. Kopp, T. Schwetz and J. Zupan, *Light dark matter in the light of CRESST-II*, *JCAP* **03** (2012) 001 [arXiv:1110.2721] [INSPIRE].

[17] M.T. Frandsen, F. Kahlhoefer, C. McCabe, S. Sarkar and K. Schmidt-Hoberg, *The unbearable lightness of being: CDMS versus XENON*, *JCAP* **07** (2013) 023 [arXiv:1304.6066] [INSPIRE].

[18] C. Savage, G. Gelmini, P. Gondolo and K. Freese, *Compatibility of DAMA/LIBRA dark matter detection with other searches*, *JCAP* **04** (2009) 010 [arXiv:0808.3607] [INSPIRE].

[19] J.M. Cline, Z. Liu and W. Xue, *An optimistic CoGeNT analysis*, *Phys. Rev.* **D 87** (2013) 015001 [arXiv:1207.3039] [INSPIRE].

[20] Q.-H. Cao, E. Ma and G. Rajasekaran, *Observing the dark scalar doublet and its impact on the standard-model Higgs boson at colliders*, *Phys. Rev.* **D 76** (2007) 095011 [arXiv:0708.2939] [INSPIRE].

[21] R. Barbieri, L.J. Hall and V.S. Rychkov, *Improved naturalness with a heavy Higgs: an alternative road to LHC physics*, *Phys. Rev.* **D 74** (2006) 015007 [hep-ph/0603188] [INSPIRE].

[22] I. Ginzburg, K. Kanishev, M. Krawczyk and D. Sokolowska, *Evolution of Universe to the present inert phase*, *Phys. Rev.* **D 82** (2010) 123533 [arXiv:1009.4593] [INSPIRE].

[23] D. Sokolowska, *Dark matter data and quartic self-couplings in inert doublet model*, *Acta Phys. Polon.* **B 42** (2011) 2237 [arXiv:1112.2953] [INSPIRE].

[24] D. Sokolowska, *Dark matter data and constraints on quartic couplings in IDM*, arXiv:1107.1991 [INSPIRE].

[25] D. Sokolowska, *Temperature evolution of physical parameters in the Inert Doublet Model*, arXiv:1104.3326 [INSPIRE].

[26] T. Hambye and M.H. Tytgat, *Electroweak symmetry breaking induced by dark matter*, *Phys. Lett.* **B 659** (2008) 651 [arXiv:0707.0633] [INSPIRE].

JHEP09(2013)055

[27] S. Kanemura, Y. Okada and E. Senaha, *Electroweak baryogenesis and quantum corrections to the triple Higgs boson coupling*, *Phys. Lett.* **B 606** (2005) 361 [hep-ph/0411354] [INSPIRE].

[28] G. Gil, P. Chankowski and M. Krawczyk, *Inert dark matter and strong electroweak phase transition*, *Phys. Lett.* **B 717** (2012) 396 [arXiv:1207.0084] [INSPIRE].

[29] J.M. Cline and K. Kainulainen, *Improved electroweak phase transition with subdominant inert doublet dark matter*, *Phys. Rev.* **D 87** (2013) 071701 [arXiv:1302.2614] [INSPIRE].

[30] T.A. Chowdhury, M. Nemevšek, G. Senjanović and Y. Zhang, *Dark matter as the trigger of strong electroweak phase transition*, *JCAP* **02** (2012) 029 [arXiv:1110.5334] [INSPIRE].

[31] E. Ma, *Verifiable radiative seesaw mechanism of neutrino mass and dark matter*, *Phys. Rev.* **D 73** (2006) 077301 [hep-ph/0601225] [INSPIRE].

[32] M. Gustafsson, J.M. No and M.A. Rivera, *The cocktail model: neutrino masses and mixings with dark matter*, *Phys. Rev. Lett.* **110** (2013) 211802 [arXiv:1212.4806] [INSPIRE].

[33] P. Agrawal, E.M. Dolle and C.A. Krenke, *Signals of inert doublet dark matter in neutrino telescopes*, *Phys. Rev.* **D 79** (2009) 015015 [arXiv:0811.1798] [INSPIRE].

[34] M. Gustafsson, E. Lundstrom, L. Bergstrom and J. Edsjo, *Significant γ lines from inert Higgs dark matter*, *Phys. Rev. Lett.* **99** (2007) 041301 [astro-ph/0703512] [INSPIRE].

[35] E.M. Dolle and S. Su, *The inert dark matter*, *Phys. Rev.* **D 80** (2009) 055012 [arXiv:0906.1609] [INSPIRE].

[36] E. Dolle, X. Miao, S. Su and B. Thomas, *Dilepton signals in the inert doublet model*, *Phys. Rev.* **D 81** (2010) 035003 [arXiv:0909.3094] [INSPIRE].

[37] L. Lopez Honorez, E. Nezri, J.F. Oliver and M.H. Tytgat, *The inert doublet model: an archetype for dark matter*, *JCAP* **02** (2007) 028 [hep-ph/0612275] [INSPIRE].

[38] C. Arina, F.-S. Ling and M.H. Tytgat, *IDM and iDM or the Inert Doublet Model and inelastic Dark Matter*, *JCAP* **10** (2009) 018 [arXiv:0907.0430] [INSPIRE].

[39] M.H. Tytgat, *The Inert Doublet Model: a new archetype of WIMP dark matter?*, *J. Phys. Conf. Ser.* **120** (2008) 042026 [arXiv:0712.4206] [INSPIRE].

[40] L. Lopez Honorez and C.E. Yaguna, *The inert doublet model of dark matter revisited*, *JHEP* **09** (2010) 046 [arXiv:1003.3125] [INSPIRE].

[41] M. Krawczyk and D. Sokolowska, *Constraining the Dark 2HDM*, arXiv:0911.2457 [INSPIRE].

[42] S. Kanemura, T. Kubota and E. Takasugi, *Lee-Quigg-Thacker bounds for Higgs boson masses in a two doublet model*, *Phys. Lett.* **B 313** (1993) 155 [hep-ph/9303263] [INSPIRE].

[43] A.G. Akeroyd, A. Arhrib and E.-M. Naimi, *Note on tree level unitarity in the general two Higgs doublet model*, *Phys. Lett.* **B 490** (2000) 119 [hep-ph/0006035] [INSPIRE].

[44] B. Swiezewska, *Yukawa independent constraints for 2HDMs with a 125 GeV Higgs boson*, arXiv:1209.5725 [INSPIRE].

[45] E. Lundstrom, M. Gustafsson and J. Edsjo, *The Inert Doublet Model and LEP II limits*, *Phys. Rev.* **D 79** (2009) 035013 [arXiv:0810.3924] [INSPIRE].

[46] M. Gustafsson, *The Inert Doublet Model and its phenomenology*, PoS(CHARGED 2010)030 [arXiv:1106.1719] [INSPIRE].

JHEP09(2013)055

[47] M. Gustafsson, S. Rydbeck, L. Lopez-Honorez and E. Lundstrom, *Status of the Inert Doublet Model and the role of multileptons at the LHC*, *Phys. Rev.* **D 86** (2012) 075019 [arXiv:1206.6316] [INSPIRE].

[48] S. Nie and M. Sher, *Vacuum stability bounds in the two Higgs doublet model*, *Phys. Lett.* **B 449** (1999) 89 [hep-ph/9811234] [INSPIRE].

[49] J. Elias-Miro et al., *Higgs mass implications on the stability of the electroweak vacuum*, *Phys. Lett.* **B 709** (2012) 222 [arXiv:1112.3022] [INSPIRE].

[50] A. Goudelis, B. Herrmann and O. Stal, *Dark matter in the Inert Doublet Model after the discovery of a Higgs-like boson at the LHC*, arXiv:1303.3010 [INSPIRE].

[51] A. Barroso, P. Ferreira, I. Ivanov and R. Santos, *Tree-level metastability bounds in two-Higgs doublet models*, arXiv:1305.1235 [INSPIRE].

[52] K. Nakamura et al., *Review of particle physics*, *J. Phys.* **G 37** (2012) 075021 [INSPIRE].

[53] A. Pierce and J. Thaler, *Natural dark matter from an unnatural Higgs boson and new colored particles at the TeV scale*, *JHEP* **08** (2007) 026 [hep-ph/0703056] [INSPIRE].

[54] L. Lopez Honorez and C.E. Yaguna, *A new viable region of the inert doublet model*, *JCAP* **01** (2011) 002 [arXiv:1011.1411] [INSPIRE].

[55] ATLAS collaboration, *Measurements of the properties of the Higgs-like boson in the two photon decay channel with the ATLAS detector using* $25\,\text{fb}^{-1}$ *of proton-proton collision data*, ATLAS-CONF-2013-012 (2013).

[56] C. Mariotti, *Recent results on higgs studies at CMS*, slides of a talk given at CERN, April 15, (2013).

[57] A. Djouadi, *The anatomy of electro-weak symmetry breaking. II. The Higgs bosons in the minimal supersymmetric model*, *Phys. Rept.* **459** (2008) 1 [hep-ph/0503173] [INSPIRE].

[58] A. Djouadi, *The anatomy of electro-weak symmetry breaking. I: the Higgs boson in the standard model*, *Phys. Rept.* **457** (2008) 1 [hep-ph/0503172] [INSPIRE].

[59] P. Posch, *Enhancement of* $h \to \gamma\gamma$ *in the two Higgs doublet model type I*, *Phys. Lett.* **B 696** (2011) 447 [arXiv:1001.1759] [INSPIRE].

[60] A. Arhrib, R. Benbrik and N. Gaur, $H \to \gamma\gamma$ *in inert Higgs doublet model*, *Phys. Rev.* **D 85** (2012) 095021 [arXiv:1201.2644] [INSPIRE].

[61] B. Swiezewska and M. Krawczyk, *Diphoton rate in the Inert Doublet Model with a* 125 *GeV Higgs boson*, arXiv:1212.4100 [INSPIRE].

[62] A. Djouadi, A. Falkowski, Y. Mambrini and J. Quevillon, *Direct detection of Higgs-portal dark matter at the LHC*, *Eur. Phys. J.* **C 73** (2013) 2455 [arXiv:1205.3169] [INSPIRE].

[63] G. Bélanger, B. Dumont, U. Ellwanger, J. Gunion and S. Kraml, *Status of invisible Higgs decays*, *Phys. Lett.* **B 723** (2013) 340 [arXiv:1302.5694] [INSPIRE].

[64] B. Dumont, *Higgs couplings after Moriond*, arXiv:1305.4635 [INSPIRE].

[65] S. Andreas, M.H. Tytgat and Q. Swillens, *Neutrinos from inert doublet dark matter*, *JCAP* **04** (2009) 004 [arXiv:0901.1750] [INSPIRE].

[66] M. Krawczyk, D. Sokolowska and B. Swiezewska, *2HDM with* Z_2 *symmetry in light of new LHC data*, *J. Phys. Conf. Ser.* **447** (2013) 012050 [arXiv:1303.7102] [INSPIRE].

JHEP09(2013)055

[67] M. Krawczyk, D. Sokolowska and B. Swiezewska, *Inert doublet model with a* 125 *GeV Higgs*, arXiv:1304.7757 [INSPIRE].

[68] A. Djouadi, O. Lebedev, Y. Mambrini and J. Quevillon, *Implications of LHC searches for Higgs-portal dark matter*, *Phys. Lett.* **B 709** (2012) 65 [arXiv:1112.3299] [INSPIRE].

[69] G. Bélanger, F. Boudjema, A. Pukhov and A. Semenov, *MicrOMEGAs3.1: a program for calculating dark matter observables*, arXiv:1305.0237 [INSPIRE].

[70] FERMI-LAT collaboration, M. Ackermann et al., *Constraining dark matter models from a combined analysis of Milky Way satellites with the Fermi Large Area Telescope*, *Phys. Rev. Lett.* **107** (2011) 241302 [arXiv:1108.3546] [INSPIRE].

[71] LAT collaboration, M. Ackermann et al., *Fermi LAT search for dark matter in γ-ray lines and the inclusive photon spectrum*, *Phys. Rev.* **D 86** (2012) 022002 [arXiv:1205.2739] [INSPIRE].

[72] J. Kopp, *Constraints on dark matter annihilation from AMS-02 results*, arXiv:1304.1184 [INSPIRE].

[73] K.N. Abazajian, P. Agrawal, Z. Chacko and C. Kilic, *Lower limits on the strengths of γ ray lines from WIMP dark matter annihilation*, *Phys. Rev.* **D 85** (2012) 123543 [arXiv:1111.2835] [INSPIRE].

[74] A. Geringer-Sameth and S.M. Koushiappas, *Exclusion of canonical WIMPs by the joint analysis of Milky Way dwarfs with Fermi*, *Phys. Rev. Lett.* **107** (2011) 241303 [arXiv:1108.2914] [INSPIRE].

JHEP09(2013)055